OPEN ACCESS
IOP Publishing | ISECAEP
Journal of Reliability Science and Engineering
J. Reliab. Sci. Eng. **2** (2026) 015002 (15pp)
https://doi.org/10.1088/3050-2454/ae4be1

Combined fatigue reliability analysis of engine turbine blade via direct probability integral method

Hui Li[1], **Pengfei Gao**[2], **Guohai Chen**[1] **and Dixiong Yang**[1,*]

[1] State Key Laboratory of Structural Analysis, Optimization and CAE Software for Industrial Equipment, School of Mechanics and Aerospace Engineering, Dalian University of Technology, Dalian 116024, People's Republic of China
[2] Shenyang Blade Times Precision Technology Co., Ltd, Shenyang 110179, People's Republic of China

E-mail: yangdx@dlut.edu.cn

Received 13 January 2026, revised 23 February 2026
Accepted for publication 2 March 2026
Published 10 March 2026

Abstract

The stochastic fatigue life and reliability evaluation for aero-engine turbine blades under complex operating conditions is a crucial yet challenging task in engine design and maintenance. In this study, a unified framework for hybrid high-, low-cycle and creep fatigue life and reliability analysis of turbine blades based on direct probability integral method (DPIM) is proposed. Firstly, the basic theories of combined high-and-low-cycle fatigue (CCF), creep–fatigue cumulative damage, and fatigue reliability are introduced. Secondly, the formulas of the mean, standard deviation, and probability density function of stochastic fatigue life are derived via the probability density integral equation. For CCF reliability analysis, an efficient hybrid time–frequency domain method is established, in which the stress power spectral density function is obtained via frequency-domain method, and the stochastic stress time histories are generated. Moreover, DPIM is utilized to perform the creep–fatigue reliability estimation of turbine blades. Finally, the high accuracy and efficiency of the proposed method are validated against direct Monte Carlo simulation (MCS) and surrogate model-based MCS. The results demonstrate that DPIM can uniformly and efficiently solve the statistical moments of stochastic combined fatigue life and fatigue reliability for turbine blades. Additionally, the significant effect of component coupling terms in combined fatigue damage on reliability is revealed.

Keywords: combined fatigue reliability analysis, engine turbine blade, high-and-low-cycle fatigue, creep–fatigue, direct probability integral method

* Author to whom any correspondence should be addressed.

1. Introduction

The fatigue failure of turbine blades is a critical concern due to cyclic loading within the harsh high-temperature, high-pressure operating environments of aircraft engines [1]. According to statistics [2], 49% of engine blade failures are caused by the fatigue failure. However, both the parameters of materials and operational loads of turbine blades present uncertainties [3, 4]. These loads can be summarized as follows: low-frequency centrifugal loads generated by the high-speed rotation, aerodynamic loads induced by gas flow on the blade, thermal loads resulting from non-uniform temperature distribution, and high-frequency dynamic excitations [5]. Consequently, it is imperative to conduct fatigue reliability analysis for the global safety assessment and cost reduction of aero-engines [6, 7].

The fatigue damage of turbine blades can be categorized into four classes [8]: low-cycle fatigue (LCF), high-cycle fatigue (HCF), combined high-and-low-cycle fatigue (CCF), and creep fatigue. At present, the most researches on fatigue damage analysis for turbine blades are predominantly based on a single damage mechanism, which is not in line with the actual situations. This is mainly due to the lack of a unified approach to dealing with the issues of high and low frequencies as well as creep fatigue. In practice, turbine blades are subject to coupled damage involving LCF, HCF, and creep–fatigue, among others, during operation. Consequently, the CCF damage and creep fatigue damage are more representative of actual engineering conditions. Nevertheless, the accurate and efficient reliability analyses of CCF and creep fatigue are paramount yet challenging tasks.

There are a series of studies on CCF analysis of mechanical and aerospace structures. Oakley and Nowell [9] proposed a fatigue life prediction method for combined high- and LCF loading considering foreign object damage. Based on strain–life curves and a damage index, Karunananda *et al* [10] established a life prediction method. Schweizer *et al* [11] presented a mechanism-based model to explain the accelerated crack growth rate leading to critical crack length. For CCF reliability analysis, Yue *et al* [12] conducted CCF reliability analysis of turbine blades by integrating the stress–strength interference theory and dynamic reliability model considering strength degradation. Then, a nonlinear cumulative damage model [13] under combined high-and-low-cycle loading was proposed by introducing a damage threshold dependent on HCF damage and material properties. Additionally, the adaptive least squares support vector machines [14] was developed to reduce computational burden of Monte Carlo simulation (MCS) in CCF reliability assessment. Gao *et al* [15] proposed a substructure-based Kriging surrogate model for fatigue life prediction and reliability assessment, which enhanced computational efficiency compared to MCS. Jiang *et al* [16] investigated the effects of stress and strength parameters on turbine blade fatigue reliability using a dynamic reliability model with the assumption of lognormal distribution for fatigue life.

On the creep–fatigue analysis, Kalyanasundaram *et al* [17] analyzed the creep rupture response of nickel-based superalloy. The creep fatigue damage of directionally solidified CM247LC superalloy was studied by Kumar *et al* [18]. For creep–fatigue reliability analysis, Zhang *et al* [19] developed a fuzzy multi-extreme response surface method for creep fatigue damage evaluation. Yun *et al* [20] proposed a reliability estimation method for combined fatigue life based on an adaptive Kriging model that defines a limit state function based on the equivalent inverse strain range, obviating the need to solve the Manson–Coffin equation. Deng *et al* [21] presented an improved Kriging-based hierarchical collaborative method, which adopts a dynamic hybrid ant colony algorithm to obtain the optimal parameters. Li *et al* [22] enhanced the accuracy of creep fatigue life prediction by extending the traditional creep fatigue interaction diagram and proposing a robust and flexible assessment method based on a three-dimensional damage interaction diagram. Gao *et al* [23] introduced a substructure-based distributed collaborative surrogate modeling method that considers the multi-source uncertainties and the nonlinearity of creep–fatigue damage interaction.

The aforementioned combined fatigue reliability analysis methods can be primarily classified into three categories: direct MCS, probabilistic distribution assumption-based approaches, and surrogate model-based approaches. Among these methods, MCS is the most versatile but suffers from low computational efficiency [24, 25]. The applicability of probabilistic distribution assumption-based approaches is limited, and the estimation accuracy is highly dependent on the form of assumed distribution. Furthermore, the accuracy of surrogate model-based approaches for strongly nonlinear dynamic problems requires further improvement. Moreover, existing methods for combined fatigue reliability analysis generally fail to simultaneously determine crucial statistical moments and probability density function (PDF) of the combined fatigue life. Consequently, the development of a more efficient and precise method is desirable [26]. Based on the principle of probability conservation, Chen and Yang [27] proposed the direct probability integral method (DPIM), which is a unified method for addressing stochastic statics and dynamics problems. DPIM can efficiently and uniformly solve linear and nonlinear, static and dynamic structural reliability analysis problems [28, 29], providing a promising tool for the fatigue reliability analysis of turbine blades [30].

On the basis of DPIM, this study proposes a novel and unified stochastic analysis framework that simultaneously determines statistical moments, PDF of combined fatigue life, and combined fatigue reliability. The main contributions of this paper are presented as follows:

(1) The formulas of the mean, standard deviation, PDF of the combined fatigue life, and reliability of engine turbine blades in input sample space are derived based on probability density integral equation (PDIE). In the context of DPIM, considering the multi-source randomness of structural parameters and excitations as well as the nonlinear interactions of components in combined fatigue failure, an

efficient and unified analysis of stochastic combined life and reliability is performed for a typical turbine blade.

(2) Since CCF problems couple LCF with random parameters and HCF under random excitations, the prohibitive computational cost of time-domain methods poses a significant challenge. This paper proposes a hybrid time–frequency domain method that combines frequency-domain analysis with a stress time history generation strategy, substantially enhancing the efficiency of CCF analysis.

(3) The nonlinear interactions between LCF and HCF and between the creep and fatigue have a significant impact on combined fatigue reliability. Fatigue damage models that neglect these interactions tend to overestimate the fatigue reliability of turbine blades, potentially leading to non-conservative designs.

The remainder of the study is organized as follows. In section 2, the theory aspects of fatigue cumulative damage, combined fatigue life and reliability are introduced. Section 3 elaborates the new procedures for computing stochastic responses and reliability of combined fatigue based on DPIM. In section 4, the accuracy and efficiency of the proposed method are validated by numerical examples, and the influence factors on uncertainty propagation are examined. Finally, some findings and insights are summarized in section 5.

2. Combined fatigue reliability of turbine blades

In this section, the combined fatigue reliability models of turbine blade are presented, in which the fatigue cumulative damage theories of CCF and creep–fatigue are different. Furthermore, due to the randomness of structural parameters and high-frequency excitations, the fatigue damage of the turbine blade becomes a random variable. Consequently, the structural fatigue failure mode is described by a limit state function incorporating random fatigue damage. Accordingly, the fatigue reliability of turbine blade can be obtained by solving the PDF of the fatigue limit state function.

2.1. Fatigue cumulative damage theory

In engineering practice, many mechanical structures service in long-term vibration environment, resulting in the insidious accumulation of fatigue damage that remains undetected during routine inspections. This damage eventually exceeds the fatigue limit of material, leading to structural fatigue failure. Based on the concept initially proposed by Palmgren, Miner developed the linear cumulative damage theory [31, 32] to address this issue. The theory depends on two key assumptions: zero-mean symmetric cyclic loading, and the linear damage proportional to the number of cycles at each stress level. Consequently, the total fatigue damage is calculated by

$$D = \sum_{i=1}^{j} D_i = \sum_{i=1}^{j} \frac{n_i}{N_i}, i = 1, 2, \ldots, j \tag{1}$$

where n_i means the number of cycles at stress level S_i, N_i denotes the fatigue life corresponding to stress level S_i according to the fatigue life prediction model, and D_i is the fatigue damage caused by the current stress level.

2.2. Combined fatigue cumulative damage models of turbine blades

There are various prediction models for fatigue damage of turbine blades under different operating conditions. However, most of these models suffer from the limitation in applicability, since no single model in existing studies can accurately predict fatigue damage for all materials and all working conditions. This subsection first reviews the LCF and HCF damage theories which are the base of the combined fatigue damage. Then, the fatigue cumulative damage models for CCF and creep–fatigue in turbine blades are introduced, respectively.

2.2.1. Low-cycle and high-cycle fatigue (LCF–HCF) damage.

Due to the high stress amplitudes, LCF damage must account for the combined effects of elastic and plastic strain. The strain-based fatigue life approach is commonly employed [33], based on the following Manson–Coffin formula [34, 35] that relates the strain to fatigue life

$$\varepsilon_a = \frac{\sigma'_f}{E}(2N_f)^b + \varepsilon'_f(2N_f)^c \tag{2}$$

where N_f represents the fatigue life under the corresponding stress level, ε_a is the total strain amplitude, E means the elastic modulus, σ'_f denotes the fatigue strength coefficient, σ'_f indicates the fatigue ductility coefficient, b is the fatigue strength exponent, and c means the fatigue ductility exponent.

The effect of asymmetric cyclic loading on structural fatigue damage is quantified using the Morrow total strain correction formula to correct for mean stress [36], which is given by

$$\left(\frac{\sigma'_f - \sigma_m}{\sigma'_f}\right)\left[\frac{\sigma'_f}{E}(2N_f)^b + \varepsilon'_f(2N_f)^c\right] = \varepsilon_a \tag{3}$$

in which σ_m denotes mean stress.

The primary characteristics of HCF are low stress amplitudes and a large number of cycles, wherein fatigue damage is attributed to elastic deformation. Consequently, HCF life prediction is commonly performed using the stress-based fatigue life approach, i.e. the *S–N* curve, which is typically expressed by the Basquin equation [2] as follows

$$\sigma_a = \sigma'_f(2N_f)^b. \tag{4}$$

The *S–N* curve is employed to describe the fatigue performance of material under cyclic loading. It is typically derived by fitting experimentally obtained data to determine its parameters. Then, the structural fatigue life can be directly computed according to the S-N curve.

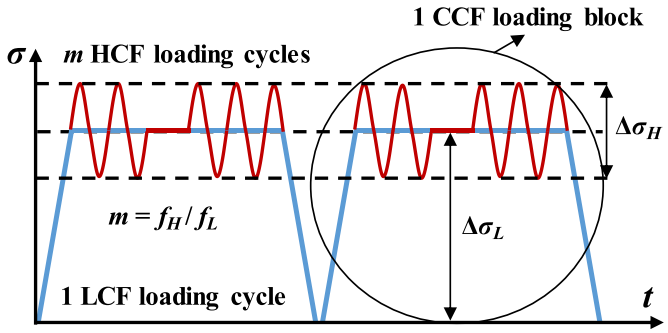

Figure 1. High-low cycle combined fatigue load spectrum.

2.2.2. CCF damage model of turbine blades. The CCF indicates such a failure mode resulting from the interaction of LCF and HCF loads. LCF, characterized by high stress amplitudes, causes elastoplastic damage, whereas the HCF, with low stress amplitudes, primarily induces elastic damage. Additionally, the coupling damage caused by the interaction between LCF and HCF should be considered in this case.

In general, the load spectrum of CCF is described by the high-cycle load amplitude $\Delta\sigma_H$, high-cycle load frequency f_H, low-cycle load amplitude $\Delta\sigma_L$, and low-cycle load frequency f_L. The CCF life is directly influenced by these four parameters [12], as illustrated in figure 1.

The prediction of the CCF life can be improved by introducing two parameters: the ratio m of high-to-low cycle, and the high-to-low stress amplitude ratio α. Additionally, since the HCF in this study accounts for stochastic stress time histories, the high-cycle stress amplitude $\Delta\sigma_H$ is not a deterministic constant; thus, it is replaced by its mean value $\Delta\bar{\sigma}_H$

$$m = \frac{f_H}{f_L} \tag{5}$$

$$\alpha = \frac{\Delta\bar{\sigma}_H}{\Delta\sigma_L}. \tag{6}$$

In the case of CCF, the linear cumulative damage theory evaluates the damage contributions from high-cycle and low-cycle loading independently, relying on linear superposition to combine the effects. In the life prediction model of CCF based on Miner's theory, the damage caused by a single combined cycle is defined as

$$D = \frac{n_{\mathrm{HCF}_i}}{N_{\mathrm{HCF}_i}} + \frac{1}{N_{\mathrm{LCF}}} \tag{7}$$

where N_{HCF_i} means the predicted HCF life under the stress with amplitude *i*, N_{LCF} denotes the predicted LCF life, and n_{HCF_i} is the number of high-cycle loading.

However, it is shown by experimental studies [37] that there is a significant coupling effect between the LCF damage dominated by plastic strain and the HCF damage dominated by elastic strain. Consequently, the estimated CCF life using Miner's rule has a considerable error, leading to unsafe predictions.

Hence, to more accurately quantify the actual damage of a material under combined high-and-low-cycle loads, the interaction damage produced by m HCF loading cycles and one LCF loading cycle is considered. Based on the coupling relationship between the high-to-low stress amplitude ratio α, and the high-to-low cycle ratio m, the coupling damage factor D_c is defined as [5]:

$$D_c = \frac{1}{(1+m)\log\left(\bar{N}_{\mathrm{HCF}}\right)^{\alpha}} \tag{8}$$

where $\bar{N}_{\mathrm{HCF}}$ represents the mean value of predicted HCF lives under stress amplitudes.

The CCF damage consists of the HCF damage, LCF damage, and the high-and-low-cycle coupling fatigue damage [5]. Thus, the total damage per combined cycle is

$$\begin{aligned} D &= \frac{n_{\mathrm{HCF}_i}}{N_{\mathrm{HCF}}} + \frac{1}{N_{\mathrm{LCF}}} + D_c \\ &= \frac{n_{\mathrm{HCF}_i}}{N_{\mathrm{HCF}}} + \frac{1}{N_{\mathrm{LCF}}} + \frac{1}{(1+m)\log\left(\bar{N}_{\mathrm{HCF}_i}\right)^{\alpha}}. \end{aligned} \tag{9}$$

In this study, equation (9) is employed to analyze the CCF damage of turbine blades. Consequently, LCF and HCF damage can be analyzed separately. Subsequently, the coupling damage factor D_c is determined using equation (8), where the distinction between high- and LCF lives is characterized by the high-to-low cycle ratio m. Finally, the total CCF damage is obtained by substituting these components into equation (9).

2.2.3. Creep–fatigue damage model of turbine blades. The creep is defined as the time-dependent and irreversible deformation phenomenon that occurs under stress levels below the yield strength. Metallic materials exhibit significant creep in high-temperature environments, and the evolution of their deformation can be divided into three typical stages. In the primary stage, the creep rate of the material gradually decreases and the creep resistance increases; during the steady-state creep stage, the creep rate tends to be stable; in the final creep stage, the creep rate increases rapidly until material fracture occurs. Engineering research usually focuses on the creep behavior in the steady-state stage.

Turbine blades operating in extreme environments are subjected to creep–fatigue interaction, where creep and LCF synergistically promote failure. Failure under creep–fatigue interaction is a common failure mode for turbine blades. The damage mechanism associated with creep–fatigue interaction is distinct from that of pure LCF or creep. For components subjected to high-temperature and high-stress environments, the creep–fatigue life is generally shorter than those under pure LCF or creep conditions [38].

Current creep experiments on metallic materials often employ accelerated life testing methods. The creep life is then evaluated by extrapolation techniques based on the acquired short-term experimental data obtained. The time–temperature parameter method utilizes the experimental time,

temperature, and stress level to calculate the material's creep life, making it a prevalent tool in engineering practice. The most commonly used time–temperature parameter method in engineering is Larson–Miller parameter method [39, 40], as written by

$$\lg \sigma_m = a_0 + a_1 P + a_2 P^2 + a_3 P^3 \tag{10}$$

$$P = \frac{T(\lg t_r + C)}{100000} \tag{11}$$

where t_r is the creep rupture time, T is the temperature of blade surface, σ_m is the stress, and a_i ($i = 0, 1, 2, 3$) are the parameters of Larson–Miller model.

The life-time fraction method is employed to describe fatigue–creep interaction damage. This approach decomposes the total damage D into the fatigue damage term D_f and the creep damage term D_{creep}. The general expression for this method is

$$D_f = \sum_{i=1}^{j} \frac{n_i}{N_{fi}} \tag{12}$$

$$D_{\text{creep}} = \sum_{i=1}^{j} \frac{t_i}{t_{ri}} \tag{13}$$

$$D = D_{\text{creep}} + D_f = \sum_{i=1}^{j} \left(\frac{t_i}{t_{ri}} + \frac{n_i}{N_{fi}} \right) \tag{14}$$

where N_{fi} is the fatigue life under a specific load, n_i is the number of cycles under the corresponding load, t_i is the actual loading time at that load, and t_{ri} is the creep rupture time under the corresponding load.

As the linear cumulative damage method fails to capture the interaction between fatigue and creep, numerous researchers proposed various modifications to the theory. Lagneberg and Attermo [41] presented a nonlinear cumulative damage model based on the time-life fraction method to represent the interaction between the fatigue and creep, i.e.

$$D = \sum_{i=1}^{j} \left(\frac{t_i}{t_{ri}} + \frac{n_i}{N_{fi}} \right) + B \left(\left(\sum_{i=1}^{j} \frac{n_i}{N_{fi}} \right) \times \left(\sum_{i=1}^{j} \frac{t_i}{t_{ri}} \right) \right)^{1/2} \tag{15}$$

where B is the coupling coefficient for creep and fatigue. The magnitude of coupling coefficient B represents the strength of the interaction between fatigue and creep. When $B > 0$, the interaction accelerates structural failure; when $B < 0$, the interaction mitigates structural failure; and when $B = 0$, indicating no interaction, the equation degrades into the linear cumulative damage formula.

2.3. Fatigue reliability of turbine blade

The fatigue reliability of a turbine blade is governed by the fatigue limit state function, which is a function of cumulative fatigue damage [42, 43]. In this study, the randomness arising from random material parameters, random parameters of fatigue damage model, and random excitations is considered. The random vector $\boldsymbol{\Theta}$ can be used to characterize the randomness from these various sources. Therefore, the fatigue limit state function (a special system response) can be expressed as

$$Z(t) = g(\boldsymbol{\Theta}, t) = 1 - \frac{D(\boldsymbol{\Theta}, t)}{D_c} \tag{16}$$

in which D_c is the damage threshold and D is the cumulative damage value.

In most cases, the damage threshold is taken as 1, and some special engineering structures or materials may use a value of 0.7. In this study, $D_c = 1$ is adopted.

Thus, the fatigue reliability for the turbine blade is given by

$$R(t) = \Pr[Z(\boldsymbol{\Theta}, t) > 0] = \int_0^{\infty} p_Z(z, t)\, \mathrm{d}z \tag{17}$$

where $p_Z(z, t)$ is the PDF of the limit state function.

3. Fatigue reliability calculation of turbine blades based on DPIM

Due to the inevitable uncertainties in structural parameters and excitations [44, 45], it is of great importance to investigate the random fatigue damage and fatigue reliability of turbine blades. This study adopts the DPIM, recently proposed by the team of authors, to address this problem. The DPIM enables efficient and unified solutions for the PDFs of responses and reliability of systems involving random parameters and (or) excitations [46–48]. Furthermore, the DPIM has been applied to the LCF and HCF reliability analysis of turbine blades [30]. In this section, the fundamental theory of DPIM is briefly introduced. Subsequently, the related formulas of CCF and creep–fatigue reliability analyses in the context of DPIM are established.

3.1. Basic idea of DPIM

For a stochastic dynamic system, the uncertainty propagation and evolution of random events obey the principle of probability conservation. It means during the propagation and evolution of random uncertainty from system input to output, the probability measure determined by the random source remains invariant [27, 49, 50]. Accordingly, there is the equation of probability conservation

$$\int_{\Omega_Z} p_Z(z, t)\mathrm{d}z = \int_{\Omega_\Theta} p_{\boldsymbol{\Theta}}(\boldsymbol{\theta})\mathrm{d}\boldsymbol{\theta} \tag{18}$$

where $p_{\boldsymbol{\Theta}}(\boldsymbol{\theta})$ means the joint PDF of random input vector; $p_Z(z,\ t)$ indicates the PDF of random response Z at the instant t; $\Omega_{\boldsymbol{\Theta}}$ denotes the input sample space or its arbitrary subset; Ω_z is the output sample space or corresponding subset, which is determined by the mapping $g(\Omega_{\boldsymbol{\Theta}}, t)$. Equation (18) expresses the principle of probability conservation [49, 50], which is a fundamental principle in probability theory and stochastic mechanics. The principle of probability conservation implies the occurrence probability of random output response at any time instant t is equal to that of random input event, and has the symmetry of time translation.

Based on equation (18), Chen and Yang [27] derived the PDIE of stochastic response that describes the law of uncertainty propagation from the input to output in static and dynamic systems. Specifically, the PDIE of stochastic response for a dynamic system can be expressed as

$$p_Z(z,t) = \int_{\Omega_{\boldsymbol{\Theta}}} \delta\left[z - g(\boldsymbol{\theta},t)\right] p_{\boldsymbol{\Theta}}(\boldsymbol{\theta})\,\mathrm{d}\boldsymbol{\theta} \tag{19}$$

in which δ indicates the Dirac delta function, which is a linear functional. PDIE is a special integral equation with generalized function, which is different from the common Fredholm and Volterra integral equations.

Note that similar to the equation of probability conservation equation (18), probability density integral equation (19) also holds true at any instant, but the PDF of response $p_Z(z,\ t)$ varies with the time. In equation (19), the system response is usually unknown, and needs to be solved numerically by the governing equation of system. Herein, the response (limit state function) of turbine blade is determined by equation (16), which is expressed as a time-varying mapping.

According to the PDIE and the sifting property of Dirac function, the integral formula over the input sample space for the mean of the stochastic dynamic response $Z(t)$ can be readily derived, namely,

$$\begin{aligned} E\left[Z(t)\right] &= \int_{\Omega_Z} z p_Z(z,t)\mathrm{d}z \\ &= \int_{\Omega_{\boldsymbol{\Theta}}} \left\{ \int_{\Omega_Z} z\delta\left[z - g(\boldsymbol{\theta},t)\right]\mathrm{d}z \right\} p_{\boldsymbol{\Theta}}(\boldsymbol{\theta})\mathrm{d}\boldsymbol{\theta} \\ &= \int_{\Omega_{\boldsymbol{\Theta}}} g(\boldsymbol{\theta},t)\, p_{\boldsymbol{\Theta}}(\boldsymbol{\theta})\mathrm{d}\boldsymbol{\theta}. \end{aligned} \tag{20}$$

Similarly, the variance of stochastic dynamic response $Z(t)$ is written by

$$\begin{aligned} D\left[Z(t)\right] &= E\left[Z(t)^2\right] - E[Z(t)]^2 \\ &= \int_{\Omega_{\boldsymbol{\Theta}}} g(\boldsymbol{\theta},t)^2 p_{\boldsymbol{\Theta}}(\boldsymbol{\theta})\mathrm{d}\boldsymbol{\theta} - \left(\int_{\Omega_{\boldsymbol{\Theta}}} g(\boldsymbol{\theta},t)\, p_{\boldsymbol{\Theta}}(\boldsymbol{\theta})\mathrm{d}\boldsymbol{\theta} \right)^2. \end{aligned} \tag{21}$$

By coupling the physical mapping with the PDIE and employing numerical methods for solution, the PDFs of the fatigue life or fatigue limit state function can be obtained. The generalized F-discrepancy based representative point selection method [51] is adopted to determine the representative points and assigned probabilities, corresponding to the integration points and weights. Then, the PDF of stochastic dynamic response is numerically expressed as

$$\begin{cases} Z_q(t) = g(\theta_q,t) \\ p_Z(z,t) = \sum\limits_{q=1}^{M} \left\{ \widehat{\delta}\left[z - g(\theta_q,t)\right] P_q \right\} \end{cases} \tag{22}$$

where $\boldsymbol{\theta}_q$ means the representative points, and P_q denotes the assigned probabilities. The assigned probability of qth representative point is obtained by the following formula

$$P_q = \int_{\Omega_{\boldsymbol{\Theta},q}} p_{\boldsymbol{\Theta}}(\boldsymbol{\theta})\,\mathrm{d}\boldsymbol{\theta} \tag{23}$$

in which $\Omega_{\boldsymbol{\Theta},q}$ is the representative subdomain, i.e. the Voronoi cell determined by the representative point $\boldsymbol{\theta}_q$

$$\Omega_{\boldsymbol{\Theta},q} = \{\boldsymbol{x} \in \mathbb{R}^s : \boldsymbol{x} - \boldsymbol{\theta}_q \leqslant \boldsymbol{x} - \boldsymbol{\theta}_j \text{ for all } j\} \tag{24}$$

where s indicates the number of random variables.

Additionally, due to the discontinuity of Dirac delta function, Gaussian function is employed in this study for smoothing the Dirac function, expressed as

$$\widehat{\delta}\left[z - g(\boldsymbol{\theta}_q,t)\right] = \frac{1}{\sqrt{2\pi}\lambda(t)} \mathrm{e}^{-[z-g(\boldsymbol{\theta}_q,t)]^2/2\lambda^2} \tag{25}$$

where the smoothing parameter $\lambda(t)$ is determined adaptively by the following formula

$$\lambda(t) = \frac{A}{M^{\frac{1}{5}}} \min_{q=1,2,\ldots,M} \left\{ \mathrm{std}\left[g(\theta_q,t)\right], \frac{\mathrm{iqr}\left[g(\theta_q,t)\right]}{1.34} \right\} \tag{26}$$

in which M refers to the number of representative points, std[·] denotes the standard deviation, iqr[·] is the interquartile range, and the smoothing factor A is taken as the values in (0, 1] and is fixed at 0.9 [28] in this study.

Similarly, the mean and variance of stochastic response can be discretized as follows

$$E\left[Z(t)\right] = \sum_{q=1}^{M} g(\boldsymbol{\theta}_q,t) P_q \tag{27}$$

$$D\left[Z(t)\right] = \sum_{q=1}^{M} g^2(\boldsymbol{\theta}_q,t) P_q - \left(\sum_{q=1}^{M} g(\boldsymbol{\theta}_q,t) P_q \right)^2. \tag{28}$$

Consequently, the DPIM enables the determination of the mean, standard deviation, and PDF of the fatigue life for turbine blades in a unified DPIM framework. Furthermore, the fatigue reliability curve can be obtained accordingly.

3.2. CCF reliability analysis based on DPIM

Based on the above, by substituting the PDF of fatigue limit state function into equation (17), the reliability of turbine blade can be formulated as

$$R(t) = \int_0^\infty p_Z(z,t)\mathrm{d}z = \int_0^\infty \int_{\Omega_\Theta} \delta\left\{z - \left[1 - \frac{D(\boldsymbol{\theta},t)}{D_c}\right]\right\} p_\Theta(\boldsymbol{\theta})\,\mathrm{d}\boldsymbol{\theta}\mathrm{d}z. \quad (29)$$

The generalized derivative of Heaviside function is Dirac delta function [52], i.e. $\delta(x) = \mathrm{d}H(x)/\mathrm{d}x$. Hence, equation (29) can be further derived as

$$R(t) = \int_{\Omega_\Theta} H\left\{\left[1 - \frac{D(\boldsymbol{\theta},t)}{D_c}\right]\right\} p_\Theta(\boldsymbol{\theta})\,\mathrm{d}\boldsymbol{\theta} \quad (30)$$

where $H[\cdot]$ is Heaviside function, i.e.

$$H\left[1 - \frac{D(\boldsymbol{\theta},t)}{D_c}\right] = \begin{cases} 1, & D_c \geqslant D(\boldsymbol{\theta},t) \\ 0, & D_c < D(\boldsymbol{\theta},t) \end{cases}. \quad (31)$$

Subsequently, the time varying fatigue reliability $R(t)$of turbine blade can be similarly solved using the representative points θ_q and the corresponding assigned probabilities P_q

$$R(t) = \sum_{q=1}^{M} H\left\{\left[1 - \frac{D(\boldsymbol{\theta}_q,t)}{D_c}\right]\right\} P_q. \quad (32)$$

The HCF damage analysis methods corresponding to the representative points can be generally classified into time-domain and frequency-domain approaches. While time-domain methods yield accurate results, they expend a prohibitive computational cost. Conversely, frequency-domain methods suffer from significant inaccuracies due to the various assumed distributions for the PDF of stress amplitude. In practice, the stress amplitude in the HCF damage analysis of turbine blades is low, indicating that the deformation remains within the elastic range. To address this issue, this study proposes a hybrid time–frequency domain method to enhance computational efficiency, as detailed in the following procedure:

Step 1: Discretize the input probability space to obtain representative points and assigned probabilities.

Step 2: Calculate the maximum equivalent elastic strain $\varepsilon_{\max}$ and the maximum equivalent stress $\sigma_{\max}$ for each representative point. Subsequently, obtain the total strain amplitude ε_a and the mean stress σ_m, determine the LCF life by Morrow total strain correction formula in equation (3).

Step 3: Calculate the HCF life.

Step 3.1: The turbine blade subjected to stationary Gaussian random excitation undergoes only elastic deformation. The power spectral density (PSD) of stress response is calculated from that of the load using frequency-domain analysis

$$S_{\sigma\sigma}(\omega) = |H(\omega)|^2 S_{FF}(\omega) \quad (33)$$

where $S_{\sigma\sigma}(\omega)$ and $S_{FF}(\omega)$ represent the PSD of stress and excitation, respectively, $H(\omega)$ is the frequency response function matrix.

Step 3.2: Utilize the spectral representation method based on random functions [53] to generate stress time histories corresponding to representative points, i.e.

$$\sigma(\boldsymbol{\Theta},t) = \sum_{k=0}^{M_\omega} \sqrt{S_{\sigma\sigma}(\omega_k)\,\Delta\omega} \cdot \left[\cos(\omega_k t) X_k + \sin(\omega_k t) Y_k\right] \quad (34)$$

X_k and Y_k are defined by random functions with two uniformly distributed random variables

$$X_k = \cos(k\theta_1) + \sin(k\theta_1), \quad Y_k = \cos(k\theta_2) + \sin(k\theta_2) \quad (35)$$

where θ_1 and θ_2 are uniformly distributed within $[-\pi, \pi]$.

Step 3.3: Adopt the rain flow counting method in time domain to calculate the HCF life of the turbine blade.

Step 4: Calculate the ratio of high-cycle to low-cycle stress amplitudes and obtain the CCF damage using equation (9).

Step 5: Based on DPIM, calculate the mean, standard deviation, and PDF of the fatigue life, and derive the CCF reliability curve.

Consequently, the hybrid time–frequency domain method not only circumvents the computationally expensive stress time history analysis but also eliminates the errors arising from assumptions regarding the PDF of stress amplitude. The flowchart of CCF reliability analysis incorporating DPIM is shown in figure 2.

3.3. Creep–fatigue reliability analysis based on DPIM

Since strain deformation in creep–fatigue damage is irreversible, the creep–fatigue reliability analysis in this study considers only LCF and creep damage. The analysis procedure based on DPIM is similar to that for CCF reliability, with the exception that the calculation models of CCF damage in Steps 3 and 4 are replaced by creep–fatigue damage calculation models. The replaced Steps 3 and 4 are displayed as follows:

Step 3: Calculate the creep–fatigue damage.

Step 3.1: Compute the maximum stress and strain responses of the turbine blade.

Step 3.2: Calculate the creep life under the corresponding stress responses using the Larson-Miller parameter method.

Step 3.3: Obtain the cumulative creep damage by using equation (15).

Step 4: Calculate the creep–fatigue damage corresponding to each representative point using the nonlinear cumulative damage model proposed by Lagneberg and Attermo [41], and determine the creep–fatigue damage life.

The whole flowchart of creep–fatigue reliability analysis based on DPIM is shown in figure 3.

4. Numerical examples

In this section, a turbine blade made of nickel-based superalloy DZ125, as shown in figure 4 [30], is considered. The turbine blade is subjected to centrifugal, aerodynamic and thermal

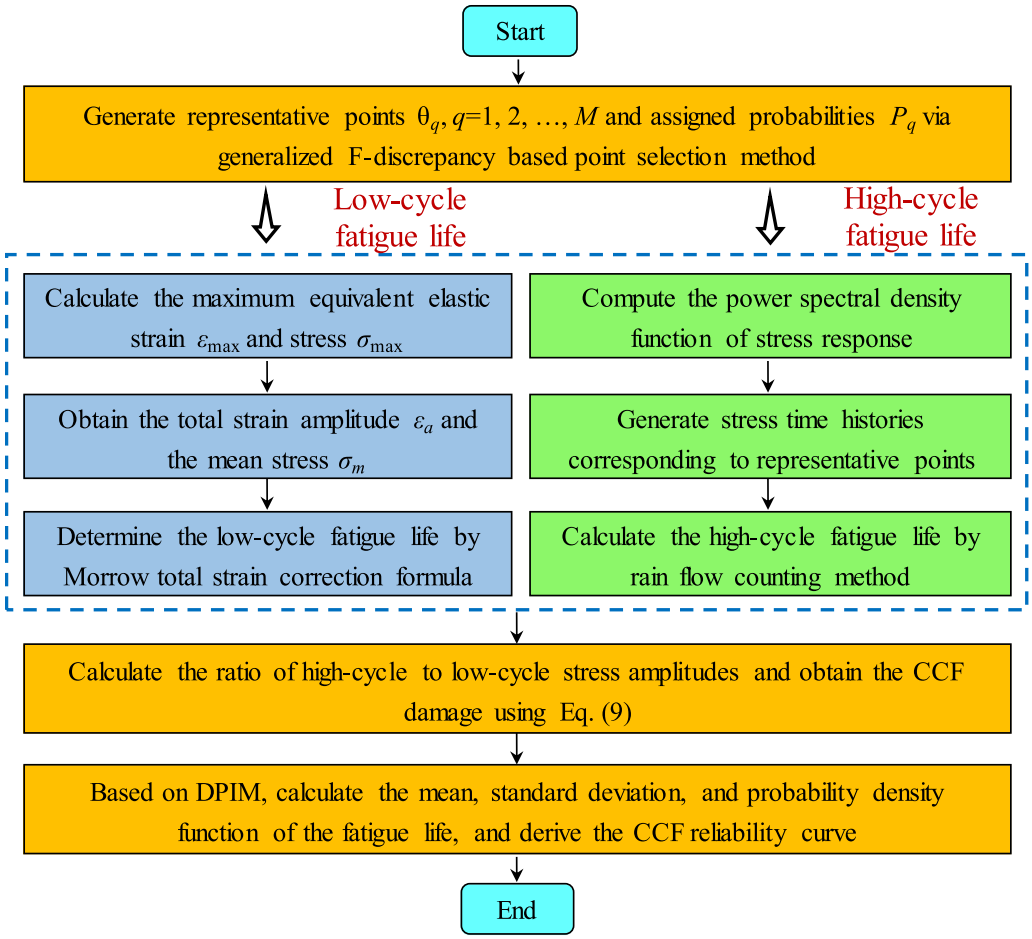

Figure 2. Flowchart of the CCF reliability analysis based on DPIM.

loads. More detailed information regarding the model can be found in [30]. The stress level of turbine blade is measured by von Mises stress.

4.1. CCF reliability of the turbine blade

The flight load spectrum associated with LCF considers an operating cycle with a running speed of $0 \rightarrow 9600 \rightarrow 0$ r min^{-1}. Additionally, this operating cycle is repeated 1000 times within a total engine operation time of 1000 h. The LCF damage analysis involves eight independent random parameters following normal distributions [14], including engine rotational speed r, Young's modulus E of the material, material density ρ, Poisson's ratio ν, fatigue strength coefficient σ_f', fatigue ductility coefficient σ_f', fatigue strength exponent b, and fatigue ductility exponent c. Among these, the first four variables are classified as aleatory uncertainties, whereas the latter four parameters represent epistemic uncertainties. The means and standard deviations of random parameters are listed in table 1.

Furthermore, the turbine blade undergoes HCF damage induced by random excitations. Specifically, the PSD of random excitation of aircraft engine acceleration is shown in figure 5. The ratio m of high-cycle to low-cycle is set to 1000 [54].

Modal analysis for turbine blade is performed to obtain the first 6 natural frequencies, as listed in table 2.

The PSD of base acceleration excitation of turbine blade illustrated in figure 5, is considered to be input, and the PSD of stress is obtained via frequency-domain analysis, as shown in figure 6.

The generated stress time histories span 1 h with a time step of 1×10^{-4} h. A set of M stress time histories is generated, where M corresponds to the number of samples in MCS or the number of representative points in DPIM.

In this subsection, direct MCS and Kriging surrogate model-based MCS are used for comparative calculation, where MCS adopts 10 000 samples, while DPIM utilizes 1050 representative points via the adaptive point selection strategy [55]. According to the solution procedure in figure 2, after partitioning the probability space, the LCF and HCF damages corresponding to each representative point are calculated and substituted into equation (9) to determine the CCF life and damage. Finally, the PDF of CCF life and reliability curve for the turbine blade are obtained by equations (22) and (32), respectively, as shown in figures 7 and 8. For comparison,

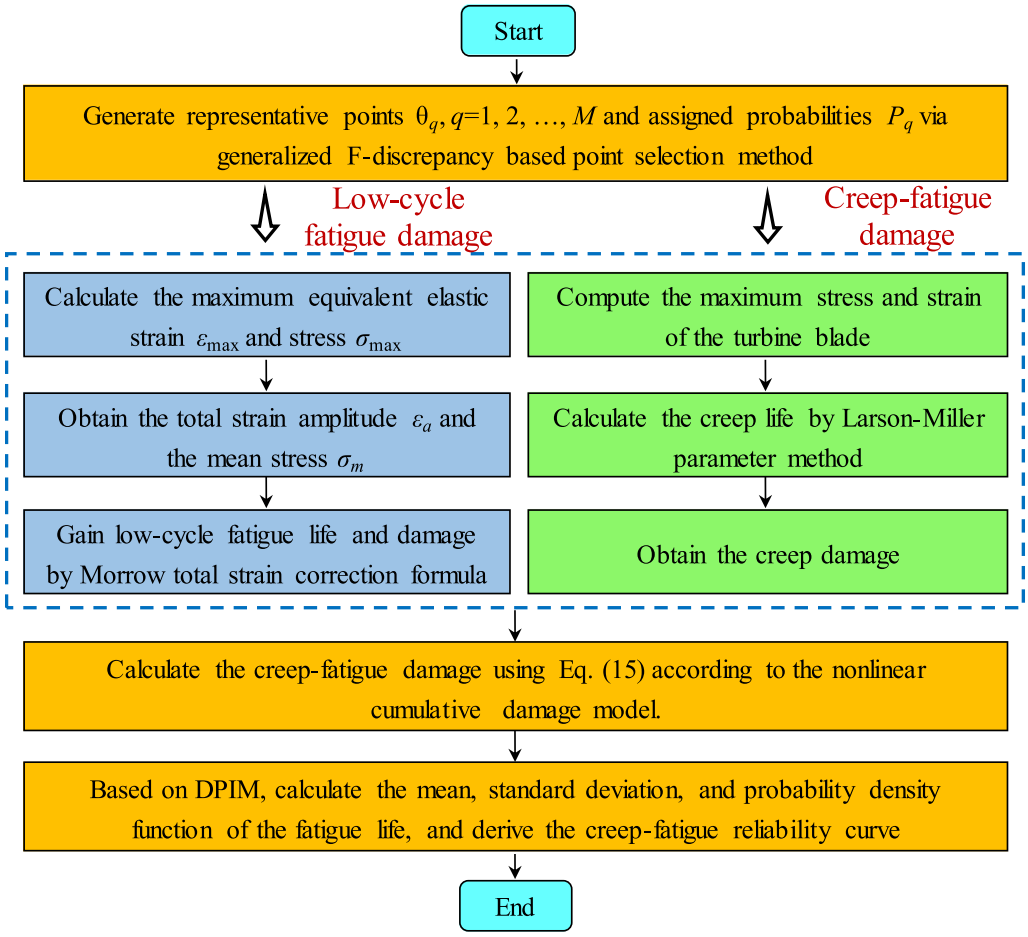

Figure 3. Flowchart of the creep–fatigue reliability analysis based on DPIM.

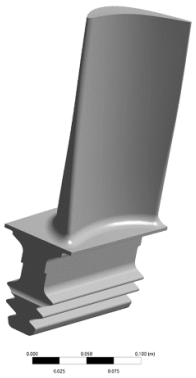

Figure 4. The turbine blade model.

the Kriging-based MCS also employs 1050 samples. In the Kriging model, the first-order polynomial is set as regression function, and the Gaussian kernel is taken as correlation model. The training samples in the Kriging model are identical to the representative points in the DPIM. In figures 7 and 8, and the horizontal axis denotes the number of operating cycles, defined as the number of repetitions of the operating state with a running speed of $0 \rightarrow 9600 \rightarrow 0$ r min^{-1}.

Furthermore, table 3 lists the comparison of results between the DPIM, Kriging model-based MCS, and direct MCS in terms of the mean, standard deviation of CCF life, and Kullback–Leibler (K–L) divergence for PDFs of the CCF life. The K–L divergence H_{K-L} is defined by

$$H_{\mathrm{K-L}} = \int_{-\infty}^{\infty} p_b(z) \ln \frac{p_b(z)}{p(z)} \mathrm{d}z \tag{36}$$

where $p_b(z)$ denotes the PDF obtained by DPIM or Kriging model-based MCS, and $p(z)$ means the PDF calculated by MCS. The K–L divergence H_{K-L} quantifies the deviation of the response PDF.

It is indicated that the accuracy of DPIM for fatigue reliability is significantly superior to Kriging model-based MCS compared to direct MCS at different numbers of cycles, as presented in table 4.

The K–L divergence between the PDFs of CCF life obtained via DPIM and direct MCS is 0.0092, which is lower than the 0.0205 for the Kriging model-based MCS. Additionally, the fatigue reliabilities at different cycle numbers indicate that DPIM possesses higher accuracy. This demonstrates that the PDF and fatigue reliability curve derived

Table 1. Distributed parameters of random variables associated with LCF.

Parameters	Distribution	Mean	Standard deviation	Parameters	Distribution	Mean	Standard deviation
r (rev min^{-1})	Normal	9600	480	σ'_f (MPa)	Normal	1381.77	27.6354
E (GPa)	Normal	99	4.95	ε'_f	Normal	0.68	0.0340
ρ (kg m^{-3})	Normal	8570	428.5	b	Normal	–0.09	0.0018
v	Normal	0.328	0.0164	c	Normal	–0.56	0.0112

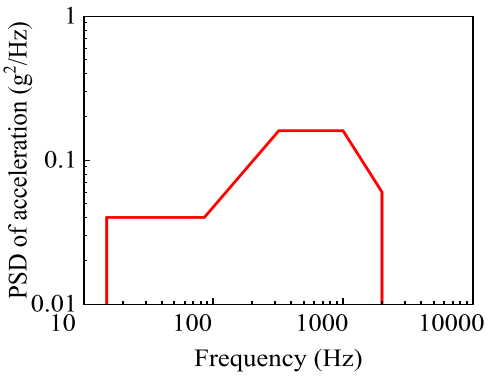

Figure 5. Power spectral density of aircraft engine acceleration.

Table 2. The first 6 natural frequencies of the turbine blade.

Order	Frequency (Hz)	Order	Frequency (Hz)
1	225.2	4	1124.6
2	698.3	5	1974.1
3	1039.4	6	2334.9

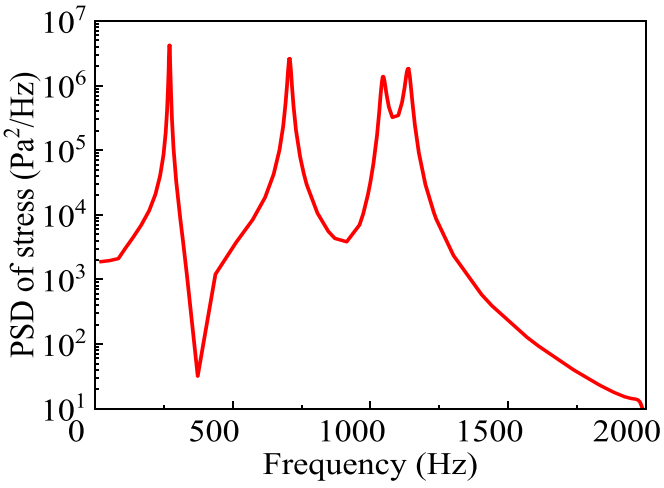

Figure 6. Power spectral density of stress response of turbine blade.

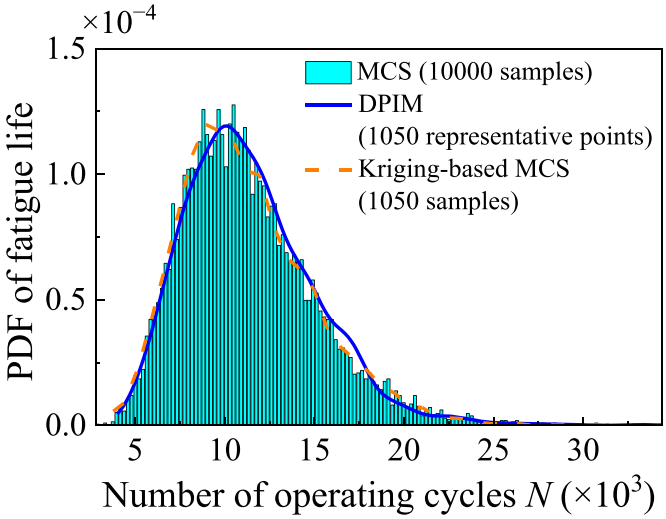

Figure 7. PDF of CCF fatigue life for the turbine blade by various methods.

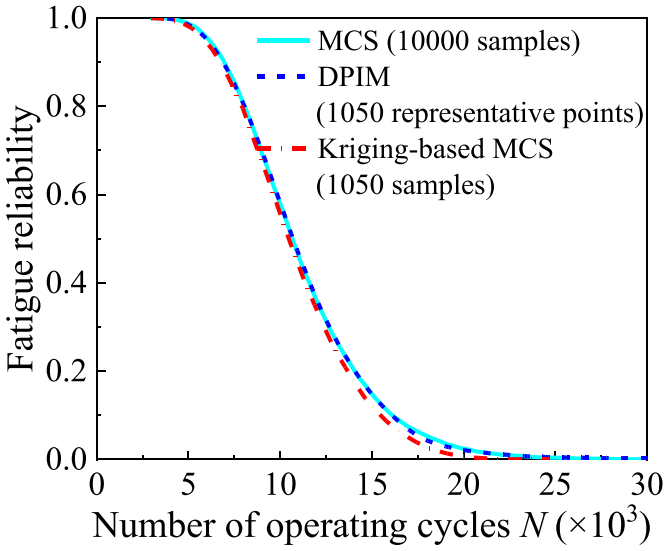

Figure 8. CCF fatigue reliability of the turbine blade by various methods.

by DPIM are closer to those of the direct MCS. Furthermore, the number of representative points in DPIM is only approximately 10% of the sample size required for direct MCS, indicating the higher computational efficiency of DPIM. Therefore, DPIM is appropriate for the stochastic CCF life and reliability analysis of turbine blades subject to the high-and-low cycle fatigue interaction.

Figure 9 illustrates the fatigue reliability curves of the turbine blade under various conditions: Case S1 incorporates the interaction between high and low cycles, Case S2 excludes this interaction, and Case S3 considers only LCF damage. By comparing with the reliability curves for LCF damage (S3) and linearly cumulative damage (S2), it is revealed that the CCF reliability (S1) is significantly lower than other. This demonstrates that LCF damage analysis or linearly cumulative fatigue damage analysis leads to an overestimation of fatigue

Table 3. Comparison of CCF fatigue life of the turbine blade considering random parameters and random excitations by using different methods.

	CCF fatigue life (N)				
	MCS	DPIM	Error	Kriging	Error
Mean	11318	11386	–0.60%	11188	1.15%
Standard deviation	3736.8	3791.9	–1.47%	3599.9	3.66%
$H_{\text{K–L}}$		0.0092		0.0205	

Table 4. Comparison of CCF fatigue reliability of the turbine blade under different cycle numbers by using different methods.

	CCF reliability $R(N)$					
Number of operating cycles N	MCS	COV	DPIM	Error	Kriging	Error
0.5×10^4	0.9868	0.12%	0.9851	0.17%	0.9812	0.57%
1×10^4	0.5723	0.86%	0.5753	–0.52%	0.5564	2.78%
1.5×10^4	0.1475	2.40%	0.1503	–1.90%	0.1212	17.83%
2×10^4	0.0247	6.28%	0.0223	9.72%	0.0168	31.98%

Note: COV means the coefficient of variation of MCS results.

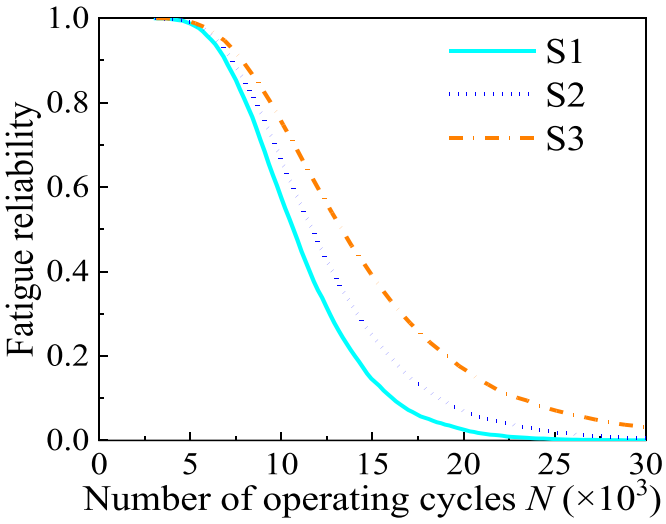

Figure 9. CCF fatigue reliability curve of the turbine blade under various conditions.

reliability for the turbine blade, potentially resulting in a hazardous design. Consequently, it is crucial to account for the nonlinear terms in high-low cycle combined fatigue analysis.

4.2. Creep–fatigue reliability of the turbine blade

The creep–fatigue reliability analysis is performed in this subsection to address LCF and creep damage. The load spectrum for LCF remains identical to that in section 4.1, while the creep damage analysis mainly incorporates the influence of the randomness in inlet temperature. The creep–fatigue reliability analysis is modeled using fourteen normally distributed independent random variables, comprising the eight variables listed in table 1 and six variables from the Larson–Miller parameter method. The variables of Larson–Miller parameter method represent epistemic uncertainties. The specific distribution parameters for these random variables are detailed in table 5. The interaction coefficient B for creep–fatigue coupling is taken as 2.8.

Similarly, MCS and Kriging surrogate model-based method are employed for comparison. MCS utilizes 10 000 samples. DPIM selects 915 representative points via the adaptive point selection strategy, while the Kriging model adopts the same number of samples as DPIM. Following the procedure in figure 3, the LCF and creep damage for each representative point are determined and substituted into equation (15) to calculate the creep–fatigue life and damage. Consequently, the PDF of the creep–fatigue life and creep–fatigue reliability are derived using equations (22) and (32), respectively, as illustrated in figures 10 and 11.

The mean, standard deviation of creep–fatigue life, and K–L divergence for the PDFs of creep–fatigue life calculated by DPIM, Kriging model-based method and MCS are summarized in table 6. The error and K–L divergence are calculated using the results of MCS as the benchmark solution. Additionally, the creep–fatigue reliabilities at different cycle numbers are shown in table 7.

The K–L divergence between the PDF of creep–fatigue life obtained by DPIM and that by MCS is 0.0039, which is lower than the 0.0112 observed for the Kriging model-based method. Furthermore, it is seen from table 7 that the calculation error of creep-reliability by DPIM is consistently lower. Consequently, DPIM demonstrates higher accuracy in calculating the statistical moments, PDF of creep–fatigue life, and creep–fatigue reliability. The computational cost of DPIM is lower, being approximately 10% of that required for MCS. Consequently, DPIM is effective for the stochastic combined fatigue life and reliability analysis of turbine blades considering creep–fatigue interaction.

Similarly, figure 12 compares the fatigue reliability curves of the turbine blade under various cases. Case S1 represents the consideration of creep–fatigue interaction, as described in

Table 5. Distributed parameters of random variables associated with creep–fatigue.

Random parameters	Distribution	Mean	Standard deviation	Random parameters	Distribution	Mean	Standard deviation
r (rev min^{-1})	Normal	9600	480	σ'_f (MPa)	Normal	1381.77	27.6354
E (GPa)	Normal	99	4.95	ε'_f	Normal	0.68	0.0340
ρ (kg m^{-3})	Normal	8570	428.5	b	Normal	–0.09	0.0018
v	Normal	0.328	0.0164	c	Normal	–0.56	0.0112
T (K)	Normal	1100	55	C	Normal	14.147	0.7074
a_0	Normal	4.2254	0.2113	a_1	Normal	–8.1926	0.4096
a_2	Normal	31.4522	1.5726	a_3	Normal	–63.8347	3.1917

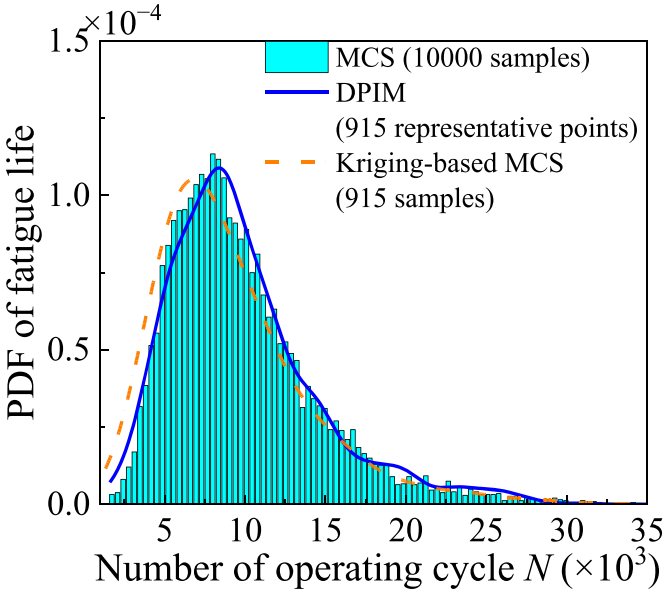

Figure 10. PDF of creep–fatigue life for the turbine blade by various methods.

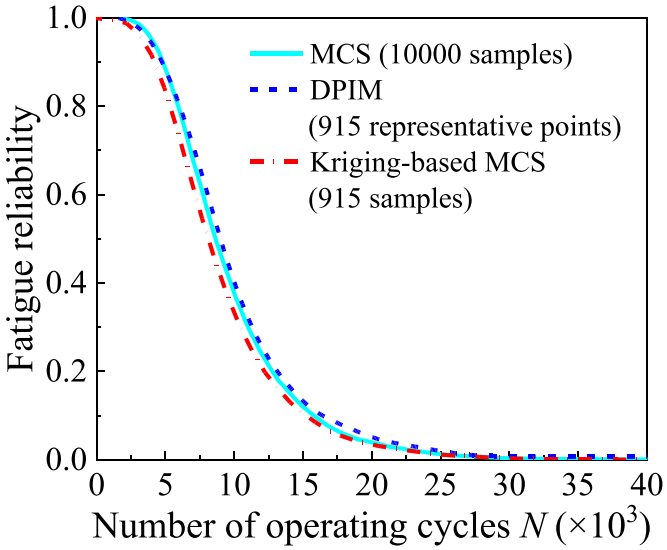

Figure 11. Creep–fatigue reliability of the turbine blade by various methods.

equation (15); Case S2 denotes the linear cumulative damage method, corresponding to equation (14); and Case S3 neglects creep damage. The results indicate that the fatigue reliability calculated for Case S1 is significantly lower than that of the other two cases, demonstrating that creep damage significantly reduces the fatigue reliability of the turbine blade. Furthermore, the linear cumulative damage method tends to overestimate fatigue reliability, which may lead to unsafe designs. Therefore, it is crucial to account for creep effects and the non-linear creep–fatigue interaction terms.

Table 6. Comparison of creep–fatigue life of the turbine blade by using different methods.

	Creep–fatigue life (N)				
	MCS	DPIM	Error	Kriging	Error
Mean	9864.9	9933.4	–0.69%	9599.6	2.69%
Standard deviation	4836.2	4827.3	0.18%	4822.8	0.28%
$H_{K\text{–}L}$		0.0039		0.0112	

Table 7. Comparison of creep–fatigue reliability of the turbine blade under different cycle numbers.

	Creep–fatigue $R(N)$					
Number of operating cycles N	MCS	COV	DPIM	Error	Kriging	Error
0.5×10^4	0.8851	0.36%	0.8830	0.24%	0.8338	5.80%
1×10^4	0.3776	1.28%	0.3950	–4.60%	0.3337	11.63%
1.5×10^4	0.1201	2.71%	0.1249	–3.98%	0.1052	12.41%
2×10^4	0.0395	4.93%	0.0436	–10.33%	0.0349	11.65%

Note: COV means the coefficient of variation of MCS results.

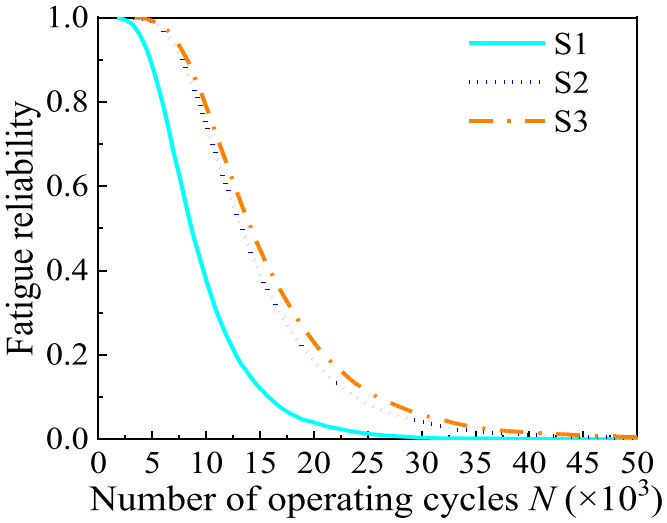

Figure 12. Creep–fatigue reliability curve of the turbine blade under various conditions.

5. Conclusions

This paper establishes a unified framework based on DPIM for the stochastic analysis of CCF, creep–fatigue life, and reliability of engine turbine blades. For CCF life and reliability analysis, a hybrid time–frequency domain method based on DPIM is proposed, which replaces the computationally expensive time-domain analysis and significantly enhances computational efficiency. Subsequently, DPIM is utilized to efficiently conduct creep–fatigue life and reliability analysis. The efficiency and accuracy of the proposed framework is verified by numerical examples. The main conclusions and insights are summarized as follows:

(1) The unified framework for stochastic combined fatigue life and reliability analyses of turbine blades based on DPIM is constructed. Utilizing the PDIE, the formulas for the mean, standard deviation, and PDF of the combined fatigue life of turbine blades in input sample space are derived which make them easy to computation, and the combined fatigue reliability is obtained. This facilitates the unified stochastic fatigue analysis of turbine blades within the framework of DPIM.

(2) The hybrid time–frequency domain method based on DPIM is proposed, significantly improving the computational efficiency of CCF fatigue reliability analysis for turbine blades. The PSD of stress for the turbine blade is calculated by frequency-domain method. Then, the stress time histories are generated by the spectral representation method. The spectral representation method demonstrates higher computational efficiency and can replace time-consuming time-domain analysis. It presents a novel and powerful tool for assessing the CCF reliability of aero-engine turbine blades.

(3) For the estimation of statistical moments, PDFs of combined fatigue life, and reliability, DPIM requires approximately 10% of the number of representative points needed for MCS. Furthermore, the computational error of DPIM is lower than that of the surrogate model-based method. The comparative study considering multi-resource randomness illustrates that, DPIM is an efficient and accurate method for assessing the combined fatigue reliability of turbine blades.

(4) The combined fatigue reliability curves of the turbine blade are compared in the presence and absence of coupling terms. The results indicate that linear cumulative method leads to overestimated reliability results, which is detrimental to the combined fatigue design of turbine blades. Therefore, it is necessary to incorporate coupling terms to ensure that the calculation results align more closely with practical engineering applications.

Finally, it is pointed out that the computational results and conclusions of this study require further experimental validation, which will be our next work in the future. Additionally, the distinction between epistemic and aleatory uncertainties

and the selection of appropriate modeling methods remain critical challenges in this field, which need to be further studied.

Acknowledgment

The supports of the National Natural Science Foundation of China (Grant Nos. 12032008, 52378484, 12572135) are much appreciated.

Data availability statement

Data will be made available on request.

Conflict of interest

The authors declare no conflict of interest.

ORCID iDs

Guohai Chen 0000-0003-4686-6929
Dixiong Yang 0000-0003-1337-8662

References

[1] Mishra R K, Thomas J, Srinivasan K, Nandi V and Raghavendra Bhatt R R 2017 Failure analysis of an un-cooled turbine blade in an aero gas turbine engine *Eng. Fail. Anal.* **79** 836–44
[2] Yan X J and Nie J X *Fatigue of Turbine Blades* 2014 Chinese Science Press
[3] Patriarca L, Beretta S, Foletti S, Riva A and Parodi S 2020 A probabilistic framework to define the design stress and acceptable defects under combined-cycle fatigue conditions *Eng. Fract. Mech.* **224** 106784
[4] O'Dowd N M, Madarshahian R, Leung M S H, Corcoran J and Todd M D 2020 A probabilistic estimation approach for the failure forecast method using Bayesian inference *Int. J. Fatigue* **142** 105943
[5] Zhu S P, Yue P, Yu Z Y and Wang Q Y 2017 A combined high and low cycle fatigue model for life prediction of turbine blades *Materials* **10** 698
[6] Song J H, Kang W H, Lee Y J and Chun J H 2021 Structural system reliability: overview of theories and applications to optimization *ASCE-ASME J. Risk Uncertain. Eng. Syst. A Civ. Eng.* **7** 03121001
[7] Wei P F, Kitahara M, Faes M G R and Beer M 2025 Probabilistic calibration of model parameters with approximate Bayesian quadrature and active machine learning *J. Reliab. Sci. Eng.* **1** 015003
[8] Wang R Z, Zhang X C, Tu S T, Zhu S P and Zhang C C 2016 A modified strain energy density exhaustion model for creep–fatigue life prediction *Int. J. Fatigue* **90** 12–22
[9] Oakley S Y and Nowell D 2007 Prediction of the combined high- and low-cycle fatigue performance of gas turbine blades after foreign object damage *Int. J. Fatigue* **29** 69–80
[10] Karunananda K, Ohga M, Dissanayake R, Siriwardane S and Chun P J 2012 New combined high and low-cycle fatigue model to estimate life of steel bridges considering interaction of high and low amplitudes loadings *Adv. Struct. Eng.* **15** 287–302
[11] Schweizer C, Seifert T, Nieweg B, von Hartrott P and Riedel H 2011 Mechanisms and modeling of fatigue crack growth under combined low and high cycle fatigue loading *Int. J. Fatigue* **33** 194–202
[12] Yue P, Ma J, Zhou C H, Zu J W and Shi B Q 2021 Dynamic fatigue reliability analysis of turbine blades under combined high and low cycle loadings *Int. J. Damage Mech.* **30** 825–44
[13] Yue P, Ma J, Huang J, Shi H and Zu J W 2021 Threshold damage-based fatigue life prediction of turbine blades under combined high and low cycle fatigue *Int. J. Damage Mech.* **150** 106323
[14] Yue P, Ma J, Dai C P, Zhang J F and Du W Y 2023 Probabilistic framework for reliability analysis of gas turbine blades under combined loading conditions *Structures* **55** 1437–46
[15] Gao H F, Zio E, Wang A E, Bai G C and Fei C W 2020 Probabilistic-based combined high and low cycle fatigue assessment for turbine blades using a substructure-based kriging surrogate model *Aerosp. Sci. Technol.* **104** 105957
[16] Jiang G J, Li Z Y, Liu J, Chen H X, Sun H H and Yue Z Y 2020 Fatigue reliability analysis of a turbine blade under CCF load *J. Fail. Anal. Prev.* **20** 1192–8
[17] Kalyanasundaram V, De Luca A, Wróbel R, Tang J, Holdsworth S R, Leinenbach C and Hosseini E 2023 Tensile and creep-rupture response of additively manufactured nickel-based superalloy CM247LC *Addit. Manuf. Lett.* **5** 100119
[18] Kumar R, Krishna E H, Patnaik S, Jayabalan B, Chatterjee D, Prasad K, Mukherjee S and Mandal S 2026 Deformation behavior and failure mechanism during in-phase and out-of-phase thermomechanical fatigue in directionally solidified CM247LC superalloy *Int. J. Fatigue* **203** 109274
[19] Zhang C Y, Yuan Z S, Wang Z, Fei C W and Lu C 2019 Probabilistic fatigue/creep optimization of turbine bladed disk with fuzzy multi–extremum response surface method *Materials* **12** 3367
[20] Yun W Y, Lu Z Z, Zhang W X and Jiang X 2021 A novel inverse strain range-based adaptive Kriging method for analyzing the combined fatigue life reliability *Struct. Multidiscip. Optim.* **64** 3311–30
[21] Deng K, Song L K, Bai G C and Li X Q 2022 Improved Kriging-based hierarchical collaborative approach for multi-failure dependent reliability assessment *Int. J. Fatigue* **160** 106842
[22] Li K S, Wang J, Fan Z C, Cheng L Y, Yao S L, Wang R Z, Zhang X C and Tu S T 2022 A life prediction method and damage assessment for creep-fatigue combined with high-low cyclic loading *Int. J. Fatigue* **161** 106923
[23] Gao H F, Wang Y H, Li Y and Zio E 2024 Distributed-collaborative surrogate modeling approach for creep-fatigue reliability assessment of turbine blades considering multi-source uncertainty *Reliab. Eng. Syst. Saf.* **250** 110316
[24] Jensen H A, Jerez D J and Valdebenito M 2020 An adaptive scheme for reliability-based global design optimization: a Markov chain Monte Carlo approach *Mech. Syst. Signal Process.* **143** 106836
[25] Acevedo C H, Valdebenito M A, González I V, Jensen H A, Faes M G R and Liu Y 2024 Control variates with splitting for aggregating results of Monte Carlo simulation and perturbation analysis *Struct. Saf.* **108** 102445
[26] Wang T, Lu D G, Dong Y, Frangopol D M and Tan Y Q 2025 Dimension-reduction integration methods for uncertainty quantification of stochastic systems: a state-of-the-art review on moments estimation *J. Reliab. Sci. Eng.* **1** 042001
[27] Chen G H and Yang D X 2019 Direct probability integral method for stochastic response analysis of static and dynamic structural systems *Comput. Methods Appl. Mech. Eng.* **357** 112612

[28] Chen G H and Yang D X 2021 A unified analysis framework of static and dynamic structural reliabilities based on direct probability integral method *Mech. Syst. Signal Process.* **158** 107783
[29] Zhu S P and Keshtegar B 2025 *Structural Reliability Analysis: Analytical Methods* (Springer)
[30] Chen G H, Gao P F, Li H and Yang D X 2025 Fatigue reliability assessment of turbine blade via direct probability integral method *Chin. J. Aeronaut.* **38** 103328
[31] Miner M A 1945 Cumulative damage in fatigue *J. Appl. Mech.* **12** 159–64
[32] Cano S, Rodríguez J, Rodríguez J M, García J C, Sierra F Z, Casolco S R and Herrera M 2019 Detection of damage in steam turbine blades caused by low cycle and strain cycling fatigue *Eng. Fail. Anal.* **97** 579–88
[33] Bartošák M, Mára V, Vražina T, Španiel M and Šulák I 2025 Low-cycle fatigue behaviour of boron-added 9% Cr martensitic steel: effects of temperature, strain rate, and strain amplitude *Int. J. Fatigue* **200** 109110
[34] Manson S S 1953 *Behavior of Materials Under Conditions of Thermal Stress* (National Advisory Committee for Aeronautics)
[35] Coffin J L F 1954 A study of the effects of cyclic thermal stresses on a ductile metal *ASME Trans.* **76** 931–49
[36] Socie D and Morrow J 1980 Review of contemporary approaches to fatigue damage analysis *Risk and Failure Analysis for Improved Performance and Reliability* ed J J Burke and V Weiss (Plenum Publication Corp) ch 8 pp 141–94
[37] Namjoshi S A and Mall S 2001 Fretting behavior of Ti-6Al-4V under combined high cycle and low cycle fatigue loading *Int. J. Fatigue* **23** 455–61
[38] Tomevenya K M and Liu S J 2018 Probabilistic fatigue-creep life reliability assessment of aircraft turbine disk *J. Mech. Sci. Technol.* **32** 5127–32
[39] Zhu X W, Cheng H H, Shen M H and Pan J P 2013 Determination of C parameter of Larson-miller equation for 15CrMo steel *Adv. Mater. Res.* **791** 374–7
[40] Jan M B and Chai M 2026 Machine learning approaches for creep rupture life prediction of metallic materials: a comprehensive review *Int. J. Press. Vessels Pip.* **219** 105690
[41] Lagneborg R and Attermo R 1971 The effect of combined low-cycle fatigue and creep on the life of austenitic stainless steels *Metall. Trans.* **2** 1821–7
[42] Ghasemi S H, Kalantari H, Abdollahikho S S and Nowak A S 2019 Fatigue reliability analysis for medial tibial stress syndrome *Mater. Sci. Eng.* **99** 387–93
[43] Zhu S P, Liu Q, Zhou J and Yu Z Y 2018 Fatigue reliability assessment of turbine discs under multi-source uncertainties *Fatigue Fract. Eng. Mater. Struct.* **41** 1291–305
[44] Shi Y, Niu L Z and Beer M 2025 Adaptive artificial neural network for uncertainty propagation *J. Reliab. Sci. Eng.* **1** 015002
[45] Zhang D Q, Zhang H F, Zhou P F, Li X A, Wang F and Han X 2025 Time-variant system reliability analysis via stochastic process discretization and most probable point trajectory approximation *J. Reliab. Sci. Eng.* **1** 025001
[46] Der Kiureghian A 2022 *Structural and System Reliability* (Cambridge University Press)
[47] Kougioumtzoglou I A, Psaros A F and Spanos P D 2024 *Path Integrals in Stochastic Engineering Dynamics* (Springer)
[48] Yang D X, Liu J L, Yu R F and Chen G H 2025 Unified framework for stochastic dynamic responses and system reliability analysis of long-span cable-stayed bridges under near-fault ground motions *Eng. Struct.* **322** 119061
[49] Syski R 1967 Stochastic differential equations *Modern Nonlinear Equations* ed T L Saaty (McGraw-Hill) ch 8
[50] Li J and Chen J B 2009 *Stochastic Dynamics of Structures* (Wiley)
[51] Chen J B, Yang J Y and Li J 2016 A GF-discrepancy for point selection in stochastic seismic response analysis of structures with uncertain parameters *Struct. Saf.* **59** 20–31
[52] Hoskins R F 2009 *Delta Functions: An Introduction to Generalised Functions* 2nd edn (Woodhead Publishing)
[53] Liu Z J, Liu W and Peng Y B 2016 Random function based spectral representation of stationary and non-stationary stochastic processes *Probab. Eng. Mech.* **45** 115–26
[54] Bai S, Huang T D, Li Y F, Lu N and Huang H Z 2023 A probabilistic fatigue life prediction method under random combined high and low cycle fatigue load history *Reliab. Eng. Syst. Saf.* **238** 109452
[55] Tao T Z, Zhao G Z, Yu Y, Huang B W and Zheng H 2022 A fully adaptive method for structural stochastic response analysis based on direct probability integral method *Comput. Methods Appl. Mech. Eng.* **396** 115066

Hui Li is a PhD student at the School of Mechanics and Aerospace Engineering, Dalian University of Technology, China. His current research interests include structural reliability, reliability sensitivity, as well as reliability-based design optimization.

Pengfei Gao is a engineer at the Shenyang Blade Times Precision Technology Co., Ltd, China. He received MSc degree from Dalian University of Technology in 2025. His research focuses on fatigue reliability analysis and design of engine turbine blades.

Guohai Chen is an assistant professor at the School of Mechanics and Aerospace Engineering, Dalian University of Technology, China. His research interests include stochastic mechanics, reliability-based design optimization of industrial equipment and engineering structures, and CAE software development.

Dixiong Yang is a professor at the School of Mechanics and Aerospace Engineering, Dalian University of Technology, China. His current research interests focus on stochastic mechanics and structural reliability, structural and multidisciplinary design optimization, seismic reduction design of buildings and bridges, and computational mechanics.